# Contribution of ammonium oxidizing archaea and bacteria to intensive nitrification during summer in Mutsu Bay, Japan.

Akari Aizawa[1], Yuka Watanabe[1], Kaori Hashioka[1], Aya Kadoya[2], Satoru Suzuki[2], Takeshi Yoshimura[1,3] Isao Kudo[1,3*]

1. Graduate School of Environmental Science, Hokkaido University, Sapporo 060-0810, Japan

2. Graduate School of Science and Engineering, and Center for Marine Environmental Studies, Ehime University, Matsuyama 790-8577, Japan

3. Faculty of Fisheries Sciences, Hokkaido University, Hakodate 041-8611, Japan

*corresponding author: Isao Kudo,

Graduate School of Environmental Science, Hokkaido University, Sapporo 060-0810, Japan.

+81-11-706-2321,

E-mail:ikudo@fish.hokudai.ac.jp

Abstract

Nitrification, in which ammonium is oxidized to nitrate via nitrite, is a regeneration process of bioavailable nitrogen. Ammonia-oxidizing archaea (AOA) and ammonia-oxidizing bacteria (AOB) carry out the ammonium oxidation. Here we measured the ammonium oxidation rates (AORs), distinguishing those of AOA ($V_A$) and AOB ($V_B$), for two years in Mutsu Bay, a subarctic semi-enclosed bay. Nitrate and ammonium were depleted in the upper layer in summer, but a high concentration of nitrate was observed at the bottom (below 40 m), of up to 7.8 μM with a strong vertical gradient within several meters of the seafloor. A High AOR of up to 0.17 μM $d^{-1}$ were observed in the bottom waters. The AOA were responsible for most of the total AOR, but the $V_B$ exceeded the $V_A$ just above the seafloor (0.3 m) in September. Removal of the suspended solids (SS) did not change the AOA's oxidation activity but eliminated the AOB's. This finding suggested that AOA were free-living whereas AOB were attached to the SS's surface. It is also suggested that the sediment was this SS's source. When ammonia mono-oxygenase, *amoA*, of AOA and AOB, was quantified, the copy number of AOA-*amoA* was an order of magnitude higher than that of AOB-*amoA* throughout the study period. A significant correlation ($p < 0.05$) was found between the AOB-*amoA* copy number and $V_B$ whereas no correlation was found between the AOA-*amoA* copy number and $V_A$, suggesting the AOA-*amoA* copy number did not always represent active cells. Ammonia oxidation was occurring near the bottom waters of Mutsu Bay during the summer, and it was accompanied by a dynamic balance reflecting the difference in the AOA's and AOB's lifestyles, free-living and particle-associated, respectively.

Keywords: Nitrification, oligotrophic bay, AOB, AOA, *amoA*

1 1. Introduction

2 Phytoplankton utilize three forms of inorganic nitrogen (N) species to support
3 their growth: nitrate ($NO_3$), nitrite ($NO_2$), and ammonium ($NH_4$). These N species are
4 supplied to the euphotic layer from the terrestrial, deep water; sedimentary sources; and
5 decomposition of detrital organic matter. During the remineralization process of organic
6 N, $NH_4$ is the first product and is further oxidized to $NO_3$. This process is called
7 nitrification. Nitrification consists of the two microbially mediated processes by which
8 $NH_4$ is oxidized through $NO_2$ to $NO_3$. Light inhibits nitrification because $NH_4$- and
9 $NO_2$-oxidizing organisms are sensitive to light (Olson, 1981). Therefore, light
10 suppresses the production of $NO_3$ by nitrification in the euphotic layer. This finding
11 indicates that $NO_3$ is produced below the euphotic layer and supplied through advection
12 and mixing into the euphotic layer (Grunde and Juniper, 2011).

13 Marine nitrifying organisms comprise ammonium-oxidizing bacteria (AOB),
14 ammonium-oxidizing archaea (AOA), and nitrite-oxidizing bacteria (NOB)(Table 1).
15 Archaea have been found to be responsible for a significant proportion of $NH_4$ oxidation
16 (Könneke et al., 2005; Wuchter et al., 2006). Species composition and distribution of
17 AOA and AOB have been studied using PCR-based techniques (Caffrey et al., 2003;
18 O'Mullan and Ward, 2005; Pedneault et al., 2014). In most studies to characterize and
19 quantify AOA and AOB, researchers have used the functional and phylogenetic marker
20 gene *amoA* (ammonia mono-oxygenase subunit A). Several studies have shown that the
21 abundance of AOA is a few orders of magnitude higher than that of AOB (Bouskill et
22 al., 2012; Newell et al., 2011; Ward and O'Mullan, 2002; Wuchter et al., 2006).

23 It has been reported that the ammonia oxidizers' abundance, rather than their
24 community structures, could explain the changes in nitrification rates (Hou et al, 2013).

However, AOA dominate in abundance, but AOB drive gross nitrification in land soil (Jia and Conrad, 2009, Sterngren et al. 2015). Therefore, concerns have arisen about not only the relationship between *amoA* gene abundance and potential nitrification rate (PNR) but also AOA's and AOB's ecological importance in nitrification (Ando et al., 2009; Baker et al., 2012; Bernhard et al., 2007). The PNR was measured ammonium oxidation rate (AOR) at a higher $NH_4$ concentration (more than ten times) than in situ concentration whereas AOR was measured at the same order of magnitude of the in situ concentration. The PNR was significantly correlated with archaeal *amoA* gene abundance but had no correlation with bacterial *amoA* gene abundance in the Yangtze Estuary, indicating AOA's importance (Zheng et al., 2014). In a few studies, researchers have described the composition of ammonium-oxidizing organisms (AOOs) in conjunction with ammonium oxidation activity at the in situ concentration level (AOR) in the marine systems.

Mutsu Bay is a semi-enclosed bay, located at the northern end of Honshu, Japan (Fig. 1). Its area and average depth were 1,667 $km^2$ and 38 m. The aquaculture of scallop (*Patinopecten yessoensis*) and other fishing activities have been performed for a long time in this bay. The bottom topography is flat, deepening gradually toward the mouth. Seawater exchange occurs through the narrow mouth (opening width, 10 km) with Tsugaru warm water. A decreasing trend of nutrient concentration (Oligotrophication) has been discovered in the last three decades with the long-term monitoring of nutrients in the bay (Kudo et al. 2014). Dissolved inorganic nitrogen (DIN: $NO_3$+$NO_2$+$NH_4$) decreased to one-third its original amount at 20 m and two-thirds at the bottom from the 1980s to the 2010s. This oligotrophication was thought to occur because the introduction of scallop aquaculture induced the acceleration of faces

origin organic matter deposition to the sediment. N seems to be a limiting nutrient of primary productivity in the bay because the N:P ratio (~10) is lower than the Redfield ratio (i.e., 16). Therefore, the nitrification process is the most important process in primary productivity in the bay. Ammonium oxidization through the microbial process is a key factor to evaluate the possibility of sustainable use for fishing grounds because ammonium oxidation is the rate-limiting step in nitrification. Further knowledge of AOA's and AOB's role in nitrification is needed in the enclosed bay environment receiving organic matter from human and aquaculture activity. We hypothesize that the role and contribution of AOA and AOB may vary responding to the environmental change in the bottom layer explaining the seasonal variation in AOR. The objectives of this study were to elucidate the seasonal variation in AOR and AOA's and AOB's relative contribution to AOR in the bottom layer of Mutsu Bay. The relative contribution was evaluated by AOR using an inhibitor of ammonium oxidation by AOB (Bianchi et al., 1997; Painter, 2011). The *amoA* gene was quantified by quantitative PCR (qPCR) targeting for AOB and AOA. The contribution of particle-associated organisms to ammonium oxidation near the bottom was also examined.

## 2. Materials and Method

### 2.1 Sampling

Water samples were collected during seven cruises in May, early September, late September, and November 2018 and July, September, and November 2019 by T/S *Ushio Maru* at N-43 (water depth: 50 m), which is located in the eastern part of Mutsu Bay (Fig. 1). Salinity, temperature, and dissolved oxygen (DO) were monitored with a Sea-Bird 19 plus CTD (Conductivity, Temperature, and Depth) sensor. Water samples

were taken from the layers 2 m, 1 m, and 0.3 m above the seafloor (hereafter referred to as B-2 m, B-1 m, and B-0.3 m, respectively). Water sampling at B-2 m and B-1 m was conducted with a horizontal X-Niskin sampler. Water near the seafloor was sampled with a triple-tube mounted undisturbed corer (Type-GS, Rigo, Tokyo, Japan) and siphoned from the overlying water of the undisturbed sediment cores. This water was a mixture of the overlying water 0 cm-30 cm above the sediment and labeled B-0.3 m.

Seawater samples for nutrient analysis were collected and stored frozen until analysis. An aliquot of sample seawater was filtered with a pre-weighed GF/F (Whatman, 25 mm diameter, pre-treated at 450 °C for 6 h) for suspended-solids (SS) measurement. The filter was stored frozen, freeze-dried, and weighed several times until a constant value was attained.

2.2 Ammonium oxidation rate (AOR) by AOA and AOB

The bottom water was transferred to a light-shaded 60-mL syringe. The sample was amended with ammonium sulphate ($(NH_4)_2SO_4$) at 3-4 μmol N $L^{-1}$. Sodium chlorite ($NaClO_3$), an inhibitor of nitrite oxidation, was added at a final concentration of 10 mmol $L^{-1}$ using a three-way stopcock to prevent its exposure to air. The samples for measuring AOR by AOA were supplemented with Allyl-thiourea (ATU), an inhibitor of ammonium oxidation by AOB, at a final concentration of 86 μmol $L^{-1}$ (=10 mg $L^{-1}$). ATU at 86 μmol $L^{-1}$ inhibits AOB but not AOA (Ginestet et al, 1998; Santoro et al, 2010). Therefore, the samples for measuring total AOR by AOA and AOB were not added to ATU. Three replicates were prepared for each condition. Incubation was conducted at the in situ temperature in darkness for 74 h. During the incubation, subsamples for nutrient analysis were taken four to five times (0, 24, 36, 48, and 72 h of

incubation) from the syringes into sterile screw spits and frozen until analysis. The control was prepared using sterilized seawater with the addition of all the chemicals mentioned above.

After the samples were thawed, and nutrients ($NH_4^+$, $NO_2^-$, $NO_3^-$) were analyzed using a QuAAtro (Bran-Luebbe, Tokyo, Japan) following Grasshoff et al. (1999).

The total AOR by AOA and AOB ($V_{A+B}$) was obtained by the slope of the time-course change in $NO_2$ concentration for each syringe without ATU. The AOR by AOA alone ($V_A$) was obtained by the slope of the time-course change in $NO_2$ concentration where the AOB ammonia oxidation inhibitor ATU was added. The difference between the two rates ($V_{A+B}$-$V_A$) was defined as the AOR by AOB ($V_B$). If the average slope of triplicate samples was not significantly different from the control (Mann-Whitney U-test, $p > 0.05$), then AOR was denoted as nd (not detected).

To evaluate the contribution of SS to AOR, an inline filtration through a 3-μm pore-size filter (Nuclepore) was conducted for the B-0.3 m waters in September 2019. The AOR was measured for the filtrate as described above.

2.3 DNA purification from filter

Subsamples were taken for gene analysis of AOA and AOB in 2018 directly from the outlet of the sampler connected to a 60-mL sterilized syringe and filtered through a Sterivex filter (Millipore, 0.2-μm pores) and stored at -80 °C. Subsamples were also taken during the incubation to measure AOR.

After the sample was thawed, the filter was removed from the Sterivex cassette and DNA was extracted following the Campbell method (Wilson, 2001). The filters were chopped into 2-mL tubes, and CTAB reagent (2.0 % CTAB, 1.0 % PVP, 1.4 M

NaCl, 20 mmol $L^{-1}$ EDTA, 100 mmol $L^{-1}$ Tris-HCl, pH 8.0) was added, followed by incubation at 65°C for 15 min and then incubation with chloroform:isoamyl alcohol = 24:1 (CI). The tubes were stirred at room temperature for 20 min and then centrifuged at 4 °C (12,500 rpm, 15 min). CI was added to the supernatant and centrifuged at 4 °C (12,500 rpm, 15 min). The supernatant was mixed with 0.3 M sodium acetate (pH 5.2); then an equal volume of isopropanol was added. This mixture was cooled at -80 °C for 2 h to precipitate DNA. DNA was precipitated by centrifugation at room temperature (13,000 rpm, 30 minutes), and the supernatant was removed by decantation. The DNA was washed with 70% ethanol and centrifuged (13,000 rpm, 5 min) at room temperature. The pelleted DNA was vacuum dried and dissolved in 50 μL of TE buffer (10 mmol $L^{-1}$ Tris-HCl, 1 mmol $L^{-1}$ EDTA, pH 8.0).

2.4 Quantitative PCR (qPCR) for *amoA*

The CFX96 Real-Time system (BioRad Laboratories) was used for qPCR analysis. The reaction solution consisted of 10 μL of SsoFast EvaGreen Supermix (BioRad), 1 μL of each primer (final concentration 500 nmol $L^{-1}$), 1 μL of sample DNA (1-5 ng), and 7 μL of sterile water to make the final volume 20 μL. The primers used were crenAMO_F and crenAMO_R for Archaean *amoA* (AOA- *amoA*) (Hallam et al., 2006) and AmoA-1F and AmoA-2R for bacterial *amoA* (AOB- *amoA*) (Rotthauwe et al., 1997) (Table 2). The qPCR was programmed to denature and activate polymerase at 95 °C for 30 s for the first cycle and programed at 95 °C for 5 s, annealing at 55 °C for 20 s (AOA-*amoA*) or 57 °C for 20 s (AOB-*amoA*), extension at 72 °C for 20 s for the second cycle. This program was performed for 39 cycles. The fluorescence for melting curves was measured in the range of 60-95 °C with a 0.5 °C increase every 5 s. Each

sample was measured three times and normalized as the number of copies per mL of test water. The confidence range of the calibration curve was $3.1x10^6$ - 3.1x10 copies $mL^{-1}$ for AOA- *amoA* and $3.8x10^6$ - 3.8x10 copies $mL^{-1}$ for AOB- *amoA*. For the standard curve, the PCR product for AOA-*amoA* and AOB-*amoA* from test water was cloned with p-GEM-T Easy vector (Promega) by TA cloning. The cloned plasmid was transformed to *E. coli* DH5α and purified with a Qiagen plasmid purification Mini kit (QIAGEN). These plasmids were used for qPCR standard templates.

## 3. Results

### 3.1 Physical and nutrient environments

The vertical profile of temperature (Fig. 2) indicated that the thermocline developed in July and September. The temperature in the bottom layer (> 40 m) was below 15 °C from May to July, and it was between 16 and 22 °C in September. The temperature in November was vertically uniform at 17 °C in 2018 and 2019.

DIN varied from 0.02 to 1.93 μM for $NH_4$, from 0.01 to 1.68 μM for $NO_2$, and from 0.02 to 7.84 μM for $NO_3$ (Fig. 3). DIN in the shallower depths (< 30 m) was low (below 1 μM). DIN concentrations in the bottom layer were highest in September. The highest $NH_4$ and $NO_2$ concentrations throughout the study period were found in the bottom layer on July 27 and September 26, 2019, at 1.9 μM and 1.7 μM, respectively. The highest $NO_3$ concentration was found in the bottom layer on September 23, 2018, at 7.8 μM. In contrast, DIN concentrations in May and November were mostly below 2 μM.

### 3.2 Ammonia oxidation rate (AOR) and contribution of AOA and AOB

The total AOR ($V_{A+B}$) at B-1 and B-2 m varied from nd to 0.10 μM $d^{-1}$ from early September 2018 to November 2019 (Fig. 4). The $V_{A+B}$ at B-0.3 m varied from 0.007 to 0.173 μM $d^{-1}$ from May 2018 to November 2019. The $V_{A+B}$ was generally high in September. The maximum $V_{A+B}$ was observed at B-0.3 m in late September 2018.

The AORs by AOA ($V_A$) and AOB ($V_B$) in the bottom layers varied from 0.04 to 0.104 μM $d^{-1}$ and from nd to 0.099 μM $d^{-1}$ from May 2018 to November 2019, respectively (Fig. 5). The $V_A$ tended to have a certain range, but $V_B$ showed the increasing trend to the seafloor.

AOA's and AOB's contribution to the total AOR in September was different at B-2 m, B-1 m, and B-0.3 m (Fig. 6). AOA's and AOB's average contribution was 86% and 14% at B-2 m, 57% and 43% at B-1 m, and 41% and 59% at B-0.3 m, respectively. Therefore, AOA contributed more than AOB at B-1 m, and AOB contributed more at B-0.3 m.

### 3.3 Contribution of suspended solids (SSs) to AOR

The concentration of SSs at B-0.3 m in September 2019 was 135 ± 13 mg $L^{-1}$. After filtration with a 3-μm filter, it dropped to 20 ± 15 mg $L^{-1}$ (Fig. 7a). The filtration eliminated 85% of SSs.

The total AOR ($V_{A+B}$) in the unfiltered water at B-0.3 m was 0.11 ± 0.037 μM $d^{-1}$. The $V_{A+B}$ in the filtered water was 0.050 ± 0.019 μM $d^{-1}$ in September 2019 (Fig. 7b). A 55% decrease in the $V_{A+B}$ was observed after filtration (t-test, $p < 0.05$). The contribution of AOB accounted for 66% of the total AOR in the unfiltered B-0.3 m water, but it was almost zero in the filtered water. However, there was no significant difference in the $V_A$ between the filtered and the unfiltered samples ($p > 0.05$).

3.4 Spatiotemporal variation of AOA and AOB copy number

The AOA-*amoA* copy number varied from nd to 3.6 x$10^4$ copies $mL^{-1}$ at B-2 m, 0.034-6.3 x$10^4$ copies $mL^{-1}$ at B-1 m, and 1.1-130 x$10^4$ copies $mL^{-1}$ at B-0.3 m from May to November 2018 whereas that of AOB-*amoA* varied between 0.017-15 x$10^2$ copies $mL^{-1}$ at B-2 m, 0.0045-2.3x$10^3$ copies $mL^{-1}$ at B-1 m, and 0.36-6.6 x$10^2$ copies $mL^{-1}$ at B-0.3 m during the same period (Fig. 8). The AOA- *amoA* and AOB- *amoA* copy numbers were larger in September in all samples except AOA- *amoA* at B-0.3 m in May. The AOB-*amoA* copy numbers were larger at B-1 m and B-2 m than at B-0.3 m. The AOA-*amoA* was 10-100 times higher than the AOB-*amoA* in all samples except at B-2 m in May 2018, when AOA-*amoA* was ns.

The AOA-*amoA* copy number after 24 h of incubation was 0.22-0.62 x$10^4$ copies $mL^{-1}$ at B-2 m, 0.58-1.89 x$10^5$ copies $mL^{-1}$ at B-1 m, and 0.01-2.39 x$10^5$ copies $mL^{-1}$ at B-0.3 m. The AOB-*amoA* copy number after 24 h of incubation was 0.16-1.82 x$10^3$ copies $mL^{-1}$ at B-2 m, 0.37-2.18 x$10^3$ copies $mL^{-1}$ at B-1 m, and 0.037-5.96 x$10^3$ copies $mL^{-1}$ at B-0.3 m. A significant correlation ($p<0.05$) was found between the AOB-*amoA* copy number after 24 h and $V_B$ whereas no correlation was found between the AOA-*amoA* copy number and $V_A$ (Fig. 9).

4. Discussion

4.1 Temporal variation of temperature and nutrients

In summer, a thermocline was observed in the bottom water. In November, the thermocline disappeared due to winter vertical mixing and the water temperature became uniform in the water column. The concentrations of $NO_2$ and $NO_3$ in the bottom

water during the observation period were highest in September in 2018 and 2019 (Fig. 3). The concentration of $NO_2$ was generally low (< 0.1 μM), but a high concentration (> 1 μM) was observed in the bottom water in September, indicating the nitrification activity was high. A high concentration of $NO_2$ was similarly observed in the bottom water of Funka Bay, located 150 km north of Mutsu Bay, when the nitrification was active in summer (Kudo et al., 2007).

4.2 Seasonal changes in AOR

The total AOR ($V_{A+B}$) in the bottom water in Mutsu Bay was measured from spring to autumn for two years. The $V_{A+B}$ showed the maximum in September in 2018 and 2019, at which the concentrations of $NO_2$ and $NO_3$ were highest. The factors affecting ammonia oxidation reactions are reported irradiance, salinity, water temperature, pH, and dissolved oxygen concentration (Horak et al., 2013, Wang et al., 2014, He et al., 2018). Of these factors, irradiance inhibits ammonia oxidation. The water depth at the sampling site was 50 m, where the euphotic zone was 40 m, judged by 1% of the surface irradiance. Therefore, the irradiance did not influence the AOR in the bottom layer. The AOR showed a negative correlation with salinity ranging from 1 to 15 in the Yangtze estuary (Zheng et al., 2014). Salinity in the bottom layer in Mutsu Bay showed a small variation, between 33 and 34. Salinity was not the main factor affecting AOR in this study area. Ammonia oxidation activity is known to decrease with extreme pH, but there was a small seasonal variation (8.1±0.1) in the seawater's pH (Mori pers. com). In addition, the dissolved oxygen concentration was high enough in the bottom waters (DO > 2 mL $L^{-1}$).

One of the suggested effective factors for seasonal change in AOR is temperature (Kim et al., 2008). The temperature dependency of nitrification with an exponential increase in activity is found over an annual cycle observation in Narragansett Bay (Berounsky and Nixon, 1990). All known nitrifying bacteria in culture are mesophiles with optimal growth around 30 °C (Bock and Koops, 1992; Koops and Möller, 1992). Water temperatures in the bottom water during the observation period were below 13 °C from May to July, and they were between 16 and 18 °C in September. The water temperature would explain why the $V_{A+B}$ was higher in September than in May. However, the water temperatures in the bottom water in November, when the $V_{A+B}$ was less than 40% of that in September, were 17 °C and 16 °C in 2018 and 2019, respectively, which were not much different from those in September. This finding suggests factors besides temperature enhanced $V_{A+B}$ and nitrification activity. We will further discuss this point in the next section.

4.2 Relationship between copy numbers and AOR, and contribution of AOA and AOB

Nakagawa et al. (2007) reported that the abundance of AOA was higher than that of AOB in the deep water of the northeast of Japan Sea. The dominance of AOA rather than AOB with one to two orders of difference in abundance was also reported in the North Sea (Wutcher et al., 2006) and off the coast of California (Santro et al., 2010). The dominance of AOA throughout the year in Mutsu Bay was consistent with these regions. The number of copies for AOA-*amoA* and AOB-*amoA* was highest in September except for AOA-*amoA* at B-0.3 m, but the number of AOA-*amoA* copies at B-0.3 m was highest in May (Fig. 9). If the number of copies for AOA-*amoA* and AOB-

*amoA* represents the abundance of these AOOs, the observed high ammonia oxidizing activity in September seemed to be strongly influenced by the biomass of related organisms.

To distinguish AOA and AOB activities, an incubation experiment was conducted using ATU, an inhibitor of AOB. Overall, the $V_A$ was responsible for more than half of the $V_{A+B}$ (Fig. 6), but the $V_B$ exceeded the $V_A$ just above the sediment (B-0.3 m). The strong vertical gradient of AOR was observed in the water column within several meters from the seafloor. The stratification that was formed in the bottom waters in September likely maintains this vertical gradient.

The AOR per copy of the *amoA* gene was calculated by dividing the AOR of AOA or AOB by the number of copies of AOA- or AOB-*amoA* in 24 h of culture in September, when the AOR was high. To perform this calculation, the number of copies per AOA cell was set to one (Walker et al., 2010; Blainey et al., 2011) and the number of copies per AOB cell was set to three (Norton et al., 1996). The AOR per cell was 0.1-4 fmol $cell^{-1}$ $d^{-1}$ and 0-16 fmol $cell^{-1}$ $d^{-1}$ for AOA and AOB, respectively. The AOR per cell was higher for AOB than for AOA when $V_B$ was detected. Wuchter et al. (2006) reported the cellular $V_A$ as 2-4 fmol $cell^{-1}$ $d^{-1}$. Santoro et al. (2010) reported the cellular $V_B$ as 0.2-1.5 fmol $cell^{-1}$ $d^{-1}$. The values obtained in the present study fell within the range of reported values.

A significant correlation ($p < 0.05$) was found between the AOB-*amoA* copy number at 24 h of incubation and $V_B$ whereas no correlation was found between the AOA-*amoA* copy number and $V_A$ (Fig. 9). No correlation was found between AOR and the abundance of AOA and AOB in the Arabian Sea and the central California current (Santoro et al., 2010; Newell et al., 2011). However, the vertical profile of AOR was

correlated with the amount of AOA-*amoA* in the Gulf of California (Beman et al., 2012). One of the possible reasons for these inconsistent results between the abundance of AOO and AOR seemed to be that in most sequence-based studies, researchers amplified DNA extracted DNA from samples, but these extracts may include DNA from not only active cells but also inactive but viable cells and inactive dead cells as well as extracellular DNA from lysed or degraded cells (Gaidos et al, 2011). Therefore, the abundance evaluated by *amoA* copies does not always relate to the oxidation activities. We conclude that not only $V_A$ and $V_B$ measurements but also *amoA* copy number assay are necessary to better understand regeneration processes of bioavailable N.

4.3 Influence of SS on the rate and contribution of ammonia oxidation

When the water at B-0.3 m was filtered with a 3-μm filter, the total AOR decreased to less than half of the AOR in the unfiltered water (Fig. 7). This decrease explained that the ammonia-oxidizing microorganisms associated with SS were partially removed by the filtration. Because the size of general archaea and bacteria (nitrifying bacteria) is about 1-2 μm, it is believed that free-living ammonia-oxidizing microorganisms (not associated with SS) pass through a filter of 3-μm pores. In addition, the contributions of AOA and AOB to the AOR differed by filtration (Fig. 7). The contribution of AOB in September 2019, when the AOR was high, accounted for 66% of the total AOR in the unfiltered B-0.3 m water, but it was almost zero in the filtered water. However, there was no significant difference in the $V_A$ between the filtered and the unfiltered samples ($p > 0.05$). This finding suggests that AOA was free-living whereas AOB was attached to the SS's surface (Fig. 10). According to Stehr et al.

(1995), there are more AOB-associated particles near the sediments than in the surface water at the mouth of the Elbe River and the abundance of AOB increases as the amount of SSs in water increases. Li et al. (2022) reported the PNR of AOA and AOB using surface sediment in the Bohai Sea and South Yellow Sea. They reported that the relative contribution of $V_A$ ranged from 21 to 100%, but more than 50% of AOB's relative contribution was found in the summer in the Bohai Sea. These studies suggest that the surface sediment was the source of this SS. Thus, the main habitat of AOB seemed in the surface sediment and the abundance of AOB increased in summer responding to the increase in $NH_4$ concentration. The particle associated AOB was supplied from the surface sediment to the bottom water through resuspension and accelerated the ammonium oxidation activities in the bottom water (Fig. 10).

## Conclusion

Ammonia oxidation activities increased in the bottom waters of Mutsu Bay during the summer and was accompanied by the dynamic balance reflecting the difference in the life state of AOA and AOB, free-living and particle-attached, respectively (Fig. 10). This high ammonia oxidation activity cannot be explained only by high water temperature during this period but is closely related to the increased biomass of AOOs. Ammonia oxidation by AOB accelerated the total ammonium oxidation activity in September. Ammonia oxidation occurs not only in the bottom water but also in the sediment surface layer when AOB is supplied to the bottom water in the form of suspended solids. Because ammonium oxidation is the rate-limiting step in the nutrient regeneration process in the bottom layer, including the sediment surface,

the elucidation of the ammonia oxidation process in this study is significant considering whether primary productivity can be maintained appropriately in the future. Furthermore, maintaining a healthy bottom-sediment environment is essential for sustainable bivalve aquaculture in the bay.

## CRediT authorship contribution statement

Akari Aizawa: Investigation, Methodology, Writing-original draft. Yuka Watanabe: Investigation, Methodology. Kaori Hashioka: Investigation, Methodology. Aya Kadoya Investigation, Methodology, Resources. Satoru Suzuki: Investigation, Methodology, Resources, Writing-review & editing. Takeshi Yoshimura: Investigation, Methodology, Writing-review & editing. Isao Kudo: Conceptualization, Funding acquisition, Investigation, Methodology, Supervision, Writing-review & editing.

## Declaration of competing interest

The authors declare that they have no known competing financial interests or personal relationships that could have appeared to influence the work reported in this paper.

Acknowledgements

We thank the captain, officers, and crew of the *T/S* Ushio Maru for their helpful assistance during sampling. We are also grateful to all members in the laboratory for sampling and analyzes. This study was supported by the Grant-in-Aid for Scientific Research No.18K05776 of the Japan Society for the Promotion of Science.

Data availability

Data will be available on request.

References

Ando, Y., Nakagawa, T., Takahashi, R., Yoshihara, K., Tokuyama, T. 2009. Seasonal changes in abundance of ammonia-oxidizing archaea and ammonia-oxidizing bacteria and their nitrification in sand of an eelgrass zone. Microbes and Environments, 24, 21-27. https://doi.org/10.1264/jsme2.ME08536

Baker, B.J., Lesniewski, R.A., Dick, G.J. 2012. Genome-enabled transcriptomics reveals archaeal populations that drive nitrification in a deep-sea hydrothermal plume. The ISME journal, 6, 2269-2279. https://doi:10.1038/ismej.2012.64

Beman, J.M., Popp, B.N., Alford, S.E. 2012. Quantification of ammonia oxidation rates and ammonia-oxidizing archaea and bacteria at high resolution in the

Gulf of California and eastern tropical North Pacific Ocean. Limnol. Oceanogr., 57, 711-726. https://doi.org/10.4319/lo.2012.57.3.0711

Bernhard, A.E., Tucker, J., Giblin, A.E., Stahl, D.A., 2007. Functionally distinct communities of ammonia-oxidizing bacteria along an estuarine salinity gradient. Environ. Microbiol. 9(6), 1439–1447. https://doi.org/10.1111/j.1462-2920.2007.01260.x.

Berounsky, V.M., Nixon, S.W. 1990. Temperature and the annual cycle of nitrification in waters of Narragansett Bay. Limnol. Oceanogr., 35, 1610-1617. https://doi.org/10.4319/lo.1990.35.7.1610

Bianchi, M., Feliatra, F., Tréguer, P., Vincendeau, M.A., Morvan, J. 1997. Nitrification rates, ammonium and nitrite distribution in upper layers of the water column and in sediments of the Indian sector of the South Ocean. Deep-Sea Res. II, 44, 1017-1032. https://doi.org/10.1016/S0967-0645(96)00109-9

Blainey, P. C., Mosier, A. C., Potanina, A., Francis, C. A. & Quake, S. R. 2011. Genome of a low-salinity ammonia-oxidizing archaeon determined by single-cell and metagenomic analysis. PLoS One 6 (2). https://doi.org/10.1371/journal.pone.0016626

Bock, E., Koops, H.P. 1992. The genus Nitrobacter and related genera. In: Balows, A., Trüper, H.G., Dworkin, M., Harder, W., Schleifer, K.H. (eds) The prokaryotes, 2nd edn, Vol. III. Springer-Verlag, New York, p2302-2309.

Bouskill, M.J., Eveillard, D., Chien, D., Jayakumar, A., Ward, B.B. 2012. Environmental factors determining ammonia-oxidizing organism distribution and diversity in marine environments. Environ. Microb., 14, 714-729. https://doi.org/10.1111/j.1462-2920.2011.02623.x

Caffrey, J.M., Harrington, N., Solem, I., Ward, B.B. 2003. Biogeochemical processes in a small California estuary. 2. Nitrification activity, community structure and role in nitrogen budgets. Mar. Ecol. Prog. Ser., 248, 27-40. https://doi:10.3354/meps248027

Gaidos, E., Rusch, A., Ilardo, M., 2011. Ribosomal tag pyrosequencing of DNA and RNA from benthic coral reef microbiota: community spatial structure, rare members and nitrogen cycling guilds. Environ. Microbiol. 13 (5), 1138–1152. https://doi.org/10.1111/j.1462-2920.2010.02392.x.

Grundle, D.S., Juniper, S.K. 2011. Nitrification from the lower euphotic zone to the sub-oxic waters of a highly productive British Columbia fiord. Mar. Chem., 126, 173-181. https://doi.org/10.1016/j.marchem.2011.06.001

Grasshoff, K., Kremling, K., Ehrhardt, M., 1999. Methods of Seawater Analysis. Wiley-VCH, Weinheim, 600 pp.

Ginestet, P., Audic, J-M., Urbain, B., Block, J.-C. 1998. Estimation of nitrifying bacterial activities by measuring oxygen uptake in the presence of the metabolic inhibitors allylthiourea and azide. Appl. Environm. Microbiol., 64, 2266-2268. https://doi.org/10.1128/AEM.64.6.2266-2268.1998

Hallam, S. J., Mincer, T., Schleper, C., Preston, C., Roberts, K., Richardson, P., DeLong, E. 2006. Pathways of carbon assimilation and ammonia oxidation suggested by environmental genomic analyses of marine Crenarchaeota. *PLoS Biol.* **4**, 520–536. https://doi.org/10.1371/journal.pbio.0040437

He, H., Zhen, Y., Mi, T.Z., Fu, L.L., Yu, Z.G., 2018. Ammonia-oxidizing archaea and bacteria differentially contribute to ammonia oxidation in sediments from adjacent waters of Rushan Bay, China. Front. Microbiol. 9, 116. https://doi.org/10.3389/fmicb.2018.00116.

Horak, R., Qin, W., Schauer, A., Armbrust, E., Ingalls, A., Moffett, J., Stahl, D., Devol, A., 2013. Ammonia oxidation kinetics and temperature sensitivity of a natural marine community dominated by Archaea. ISME J. 7, 2023–2033. https://doi.org/10.1038/ismej.2013.75

Hou, J., Song, C.L., Cao, X.Y., Zhou, Y.Y., 2013. Shifts between ammonia-oxidizing bacteria and archaea in relation to nitrification potential across trophic gradients in two large Chinese lakes (Lake Taihu and Lake Chaohu). Water Res. 47 (7), 2285–2296. https://doi.org/10.1016/j.watres.2013.01.042.

Jia, Z.J., Conrad, R., 2009. Bacteria rather than archaea dominate microbial ammonia oxidation in an agricultural soil. Environ. Microbiol. 11, 1658–1671. https://doi.org/10.1111/j.1462-2920.2009.01891.x.

Kim, J.-H., Guo, X., Park, H.–S. 2008. Comparison study of the effects of temperature and free ammonia concentration on nitrification and nitrite accumulation. Process Biochem., 43, 154-160. https://doi.org/10.1016/j.procbio.2007.11.005

Könneke, M., Bernhard, A.E., de la Torre, J.T., Walker, C.B., Waterbury, J.B., Stahl, D.A. 2005. Isolation of an autotrophic ammonia-oxidizing marine archaeon. Nature, 437, 543-546. https://doi.org/10.1038/nature03911

Koops, H.P., Möller, U.C. 1992. The lithotrophic ammonia-oxidizing bacteria. In: Balows, A., Trüper, H.G., Dworkin, M., Harder, W., Schleifer, K.H. (eds.) The prokaryotes, 2nd edn., Vol. III. Springer-Verlag, New York, p2625-2337.

Kudo, I., Yoshimura, T., Lee, C.W., Yanada, M., Maita, Y. 2007. Nutrient regeneration at bottom after a massive spring bloom in a subarctic coastal environment,

Funka Bay, Japan. J. Oceanogr., 63, 791-801. https://doi.org/10.1007/s10872-007-0067-9

Kudo, I., Yoshimura, M., Hashioka, K., Adachi, T., Isoda, Y. 2014. Impact of bivalve culture on oligotrophication in Mutsu Bay. Bull. Coast. Oceanogr., 52, 83-92. In Japanese with English abstract. https://doi.org/10.32142/engankaiyo.52.1_83

Li, M., He, H., Mi, T., Zhen, Y. 2022. Spatiotemporal dynamics of ammonia-oxidizing archaea and bacteria contributing to nitrification in sediments from Bohai Sea and South Yellow Sea, China. Sci. Tot. Environ., 825, 153972. https://doi.org/10.1016/j.scitotenv.2022.153972

Nakagawa, T., Mori, K., Kato, C., Takahashi, R., Tokuyama, T. 2007. Distribution of cold-adapted ammonia-oxidizing microorganisms in the deep ocean of the northeastern Japan Sea. Microb. Environ., 22, 365-372. https://doi.org/10.1264/jsme2.22.365

Newell, S.E., Babbin, A.R., Jayakumar, A., Ward, B.B. 2011. Ammonia oxidation rates and nitrification in the Arabian Sea. Global Biogeochem. Cycles, 25, GB4016. https://doi.org/10.1029/2010GB003940

Norton, J. M., Low, J. M. & Klotz, M. G. 1996. The gene encoding ammonia monooxygenase subunit A exists in three nearly identical copies in *Nitrosospira* sp.

NpAV. FEMS Microbiol. Lett. 139, 181–188. https://doi.org/10.1111/j.1574-6968.1996.tb08200.x

Olson, R.J. 1981. $^{15}N$ tracer studies of the primary nitrite maximum. J. Mar. Res., 39, 203-226.

O'Mullan, G.D., Ward, B.B. 2005. Relationship of temporal and spatial variabilities of ammonia-oxidizing bacteria to nitrification rates in Monterey Bay, California. Appl. Environ. Microbiol., 71, 697-705. https://doi.org/10.1128/AEM.71.2.697-705.2005

Painter, S.C. 2011. On the significance of nitrification with the euphotic zone of the subpolar North Atlantic (Iceland basin) during summer 2007. J. Mar. Sys., 88, 332-335. https://doi.org/10.1016/j.jmarsys.2011.05.001

Pedneault, E., Galand, P.E., Potvin, M., Tremblay, J.É., Lovejoy, C. 2014. Archaeal amoA and ureC genes and their transcriptional activity in the Arctic Ocean. Scientific reports, 4, 4661. https://doi.org/10.1016/j.jmarsys.2011.05.001

Rotthauwe, J., Witzel, K., Liesack, W. 1997. The Ammonia Monooxygenase Structural Gene amoA as a Functional Marker: Molecular Fine-Scale Analysis of Natural Ammonia-Oxidizing Populations. *Appl. Environ. Microbiol.,* **63**, 4704-4712. https://doi.org/10.1128/aem.63.12.4704-4712.1997

Santoro, A.E., Casciotti, K.L., Francis, C.A. 2010. Activity, abundance and diversity of nitrifying archaea and bacteria in the central California Current. Environ. Microbiol., 12, 1989-2006. https://doi.org/10.1111/j.1462-2920.2010.02205.x

Stehr, G., Böttcher, B., Dittberner, P., Rath, G. & Koops, H. P. 1995. The ammonia-oxidizing nitrifying population of the River Elbe estuary. FEMS Microbiol. Ecol. 17, 177–186. https://doi.org/10.1111/j.1574-6941.1995.tb00141.x

Sterngren, A.E., Hallin, S. Bengtson, P. 2015. Archaeal ammonia oxidizers dominate in numbers, but bacteria drive gross nitrification in N-amended grassland soil. Front. In Microb.,6, 1350. https://doi.org/10.3389/fmicb.2015.01350

Thamdrup, B., Fleischer, S. 1998. Temperature dependence of oxygen respiration, nitrogen mineralization, and nitrification in Arctic sediments. Aquat. Microb. Ecol., 15, 191-199. https//doi.org/10.3354/ame015191

Walker, C., De La Torre, J., Klotz, M., Urakawa, H., Pinel, N., Arp, D., Brochier-Armanet, C., Chain, P., Chan, P., Gollabgir, A., Hemp, J., Hügler, M., Karr, E., Könneke, M., Shin, M., Lawton, T., Lowe, T., Martens-Habbena, W., Sayavedra-Soto, L., Lang, D., Sievert, S., Rosenzweig, A., Manning, G., Stahl, D. 2010. *Nitrosopumilus maritimus* genome reveals unique mechanisms for nitrification and

autotrophy in globally distributed marine crenarchaea. Proc. Natl. Acad. Sci. U. S. A. 107, 8818–8823. https://doi.org/10.1073/pnas.0913533107

Wang, Y. F., Gu, J. D. 2014. Effects of allylthiourea, salinity, and pH on ammonia/ammonium-oxidizing prokaryotes in mangrove sediment incubated in laboratory microcosms. Appl. Microbiol. Biotechnol. 98, 3257–3274. https://doi.org/10.1007/s00253-013-5399-3

Ward, B.B., O'Mullan, G.D. 2002. Worldwide distribution of *Nitrosococcus oceani*, a marine ammonia-oxidizing gamma-proteobacterium, detected by PCR and sequencing of 16S rRNA and amoA genes. Appl. Environ. Microbiol., 68, 4153–4157. https://doi.org/10.1128/AEM.68.8.4153-4157.2002

Wilson, K. 2001. Preparation of genomic DNA from bacteria. Current protocols in molecular biology. https://doi.org/10.1002/0471142727.mb0204s56

Wutchter, C., Abbas, B., Coolen, M.J.L., Herfort, L., van Bleijswijk, J., Timmers, P., Strous, M., Teira, E., Herndl, G.J., Middelburg, J.J., Schouten, S., Sinninghe Damsté, J.S. 2006. Archaeal nitrification in the ocean. Proc. Natl. Acad. Sci. USA, 103, 12317–12322. https://doi.org/10.1073/pnas.0600756103

Zheng, Y.L., Hou, L.J., Newell, S., Liu, M., Zhou, J.L., Zhao, H., et al., 2014. Community dynamics and activity of ammonia-oxidizing prokaryotes in intertidal

1 sediments of the Yangtze estuary. Appl. Environ. Microbiol. 80 (1), 408–419.

2 https://doi.org/10.1128/aem.03035-13

3

Figure legends

Figure 1 Map showing sampling location (N-43) in Mutsu Bay.

Figure 2 Temperature profiles at N-43 in 2018 and 2019.

Figure 3 DIN ($NH_4$, $NO_2$, and $NO_3$) profiles at N-43 in 2018 and 2019. Shaded area designates concentration for each DIN spices.

Figure 4 Spatial and temporal changes in ammonia oxidation rate (AOR) in 2018 and 2019. Error bar indicates standard error. NS = not sampled; ND = not detected.

Figure 5 Spatial and temporal changes in ammonia oxidation rate (AOR) by AOB ($V_B$) and AOA ($V_A$) in 2018 and 2019. Error bar indicates standard error. NS = not sampled; ND = not detected.

Figure 6 Relative contribution of $V_A$ and $V_B$ to the total AOR in September 2018 and 2019.

Figure 7 Change in the amount of SSs for unfiltered and a 3-μm filtered water (a) and change in $V_B$ and $V_A$ for unfiltered and a 3-μm filtered water (b). Error bar indicates standard error.

Figure 8 Spatial and temporal changes in abundances of AOA-*amoA* and AOB-*amoA* in 2018. Error bar indicates standard error. NS = not sampled.

Figure 9 Relationship between AOA-*amoA* abundance at 24 h and $V_A$ (a) and that between AOB-*amoA* abundance at 24 h and $V_B$.

Figure 10 Scheme explaining the role of AOA and AOB in the bottom water.

1

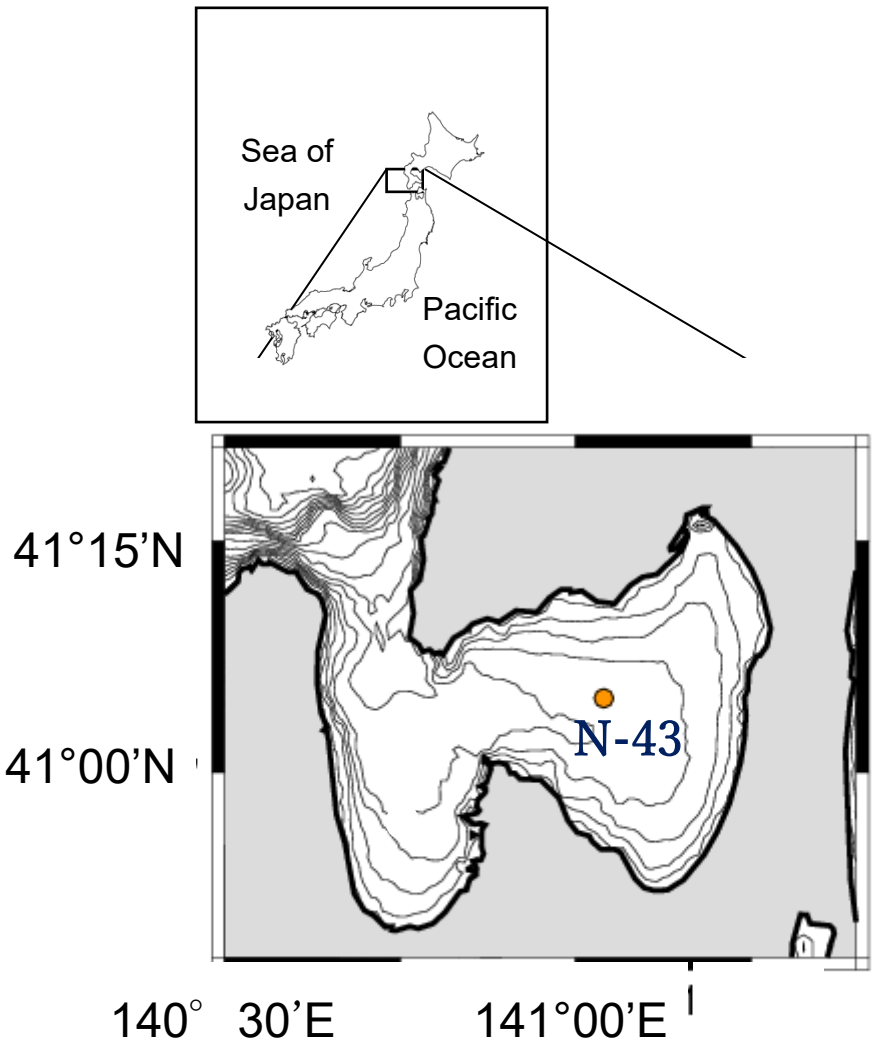


Fig. 1

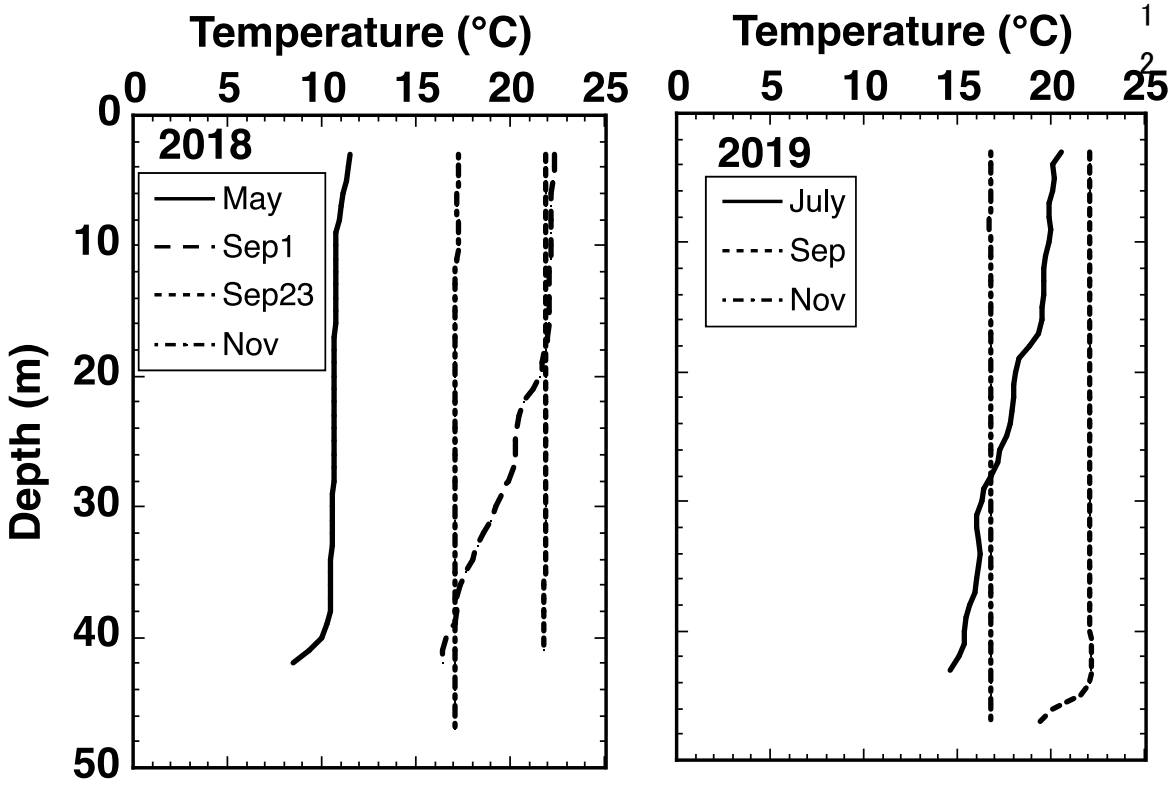
Temperature (°C)
0 5 10 15 20 25
0
10
20
30
40
50
Depth (m)
2018
May
Sep1
Sep23
Nov
Temperature (°C)
0 5 10 15 20 25
2019
July
Sep
Nov

Fig. 2

1

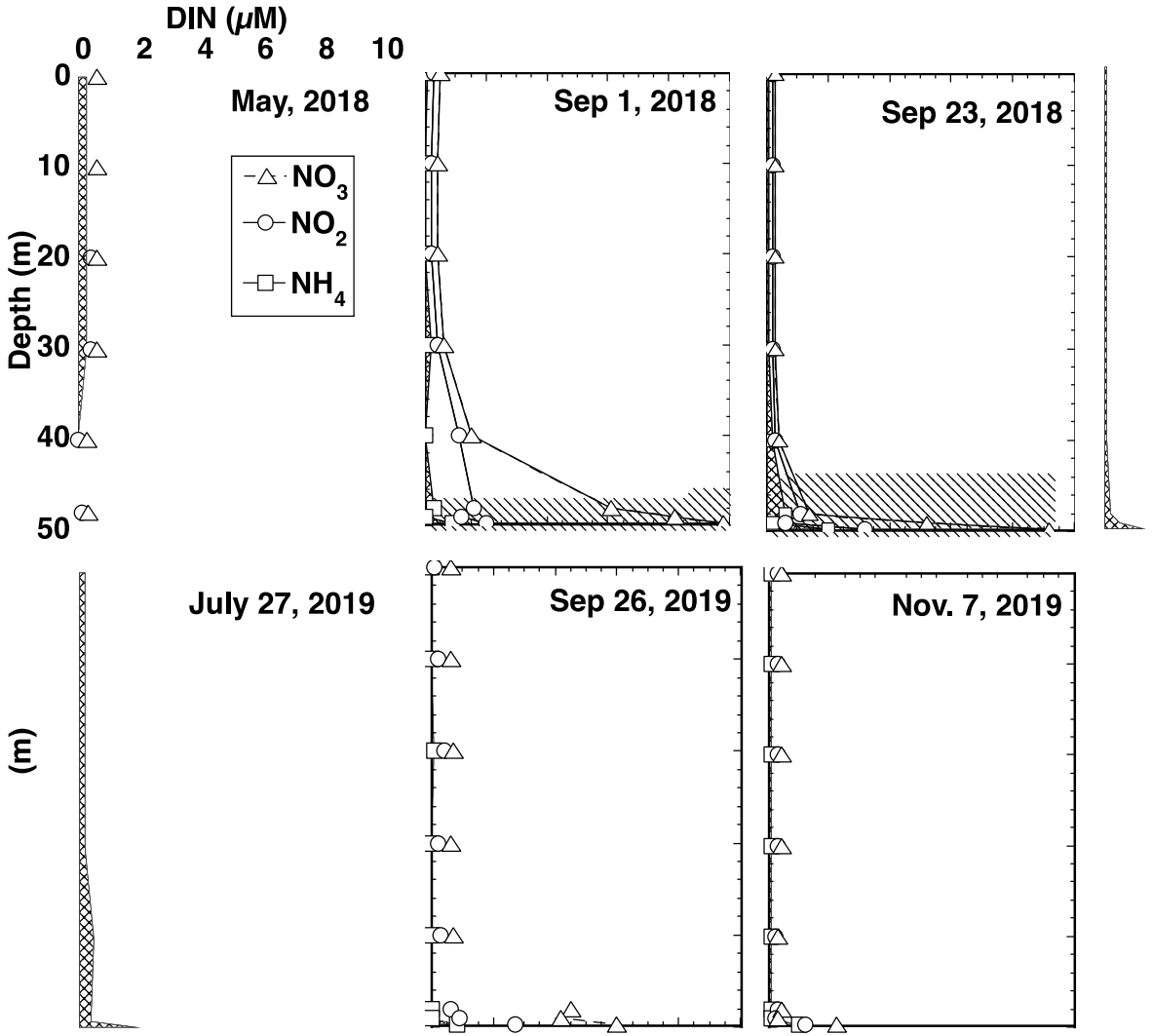
DIN (μM)
0 2 4 6 8 10
0
10
20
30
40
50
Depth (m)
May, 2018
NO3
NO2
NH4
Sep 1, 2018
Sep 23, 2018
2018
July 27, 2019
Sep 26, 2019
Nov. 7, 2019
(m)

Fig. 3

1

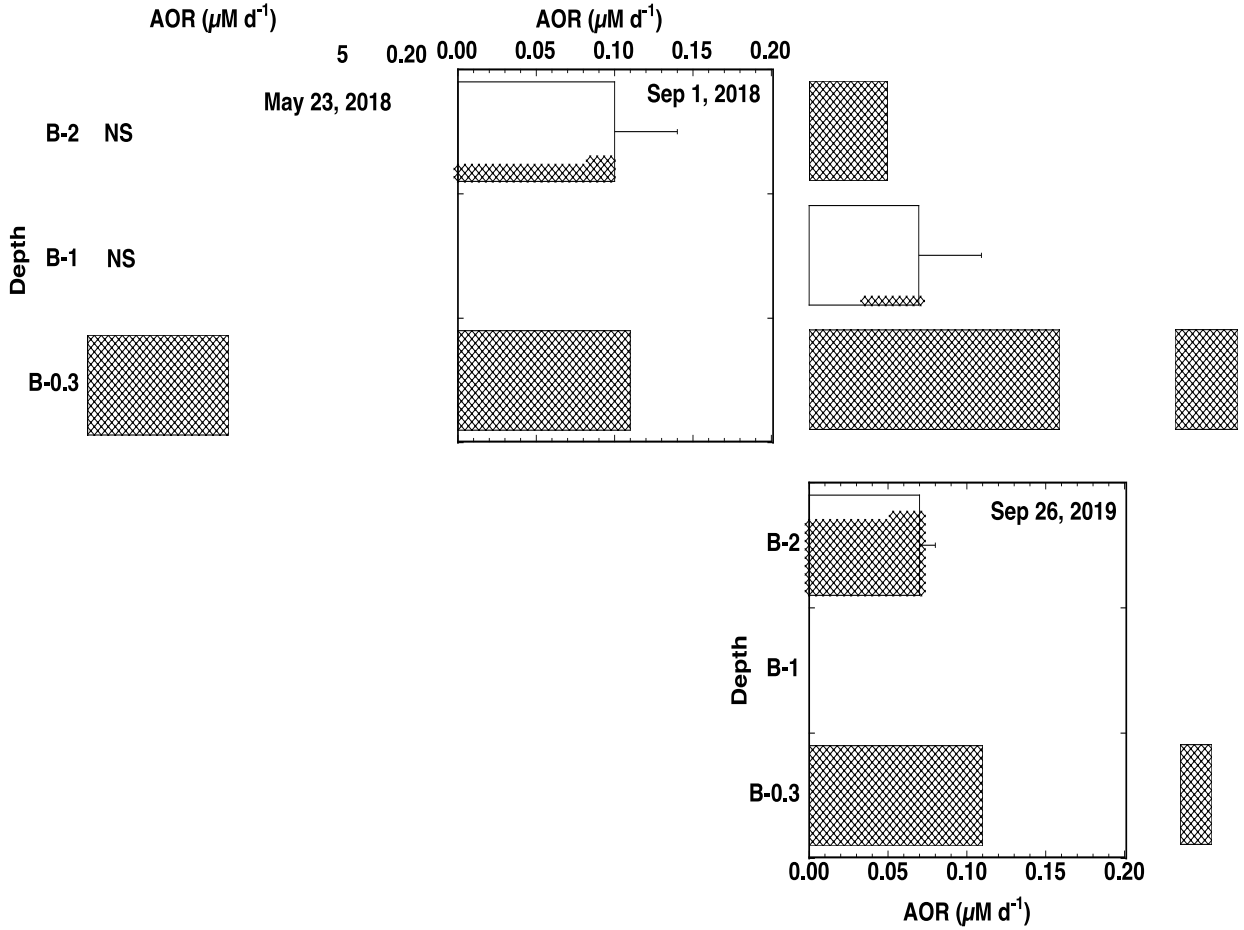
AOR (μM d-1)
AOR (μM d-1)
5
0.20
0.00
0.05
0.10
0.15
0.20
May 23, 2018
Sep 1, 2018
B-2
NS
Depth
B-1
NS
B-0.3
Sep 26, 2019
B-2
Depth
B-1
B-0.3
0.00
0.05
0.10
0.15
0.20
AOR (μM d-1)

Fig. 4

1

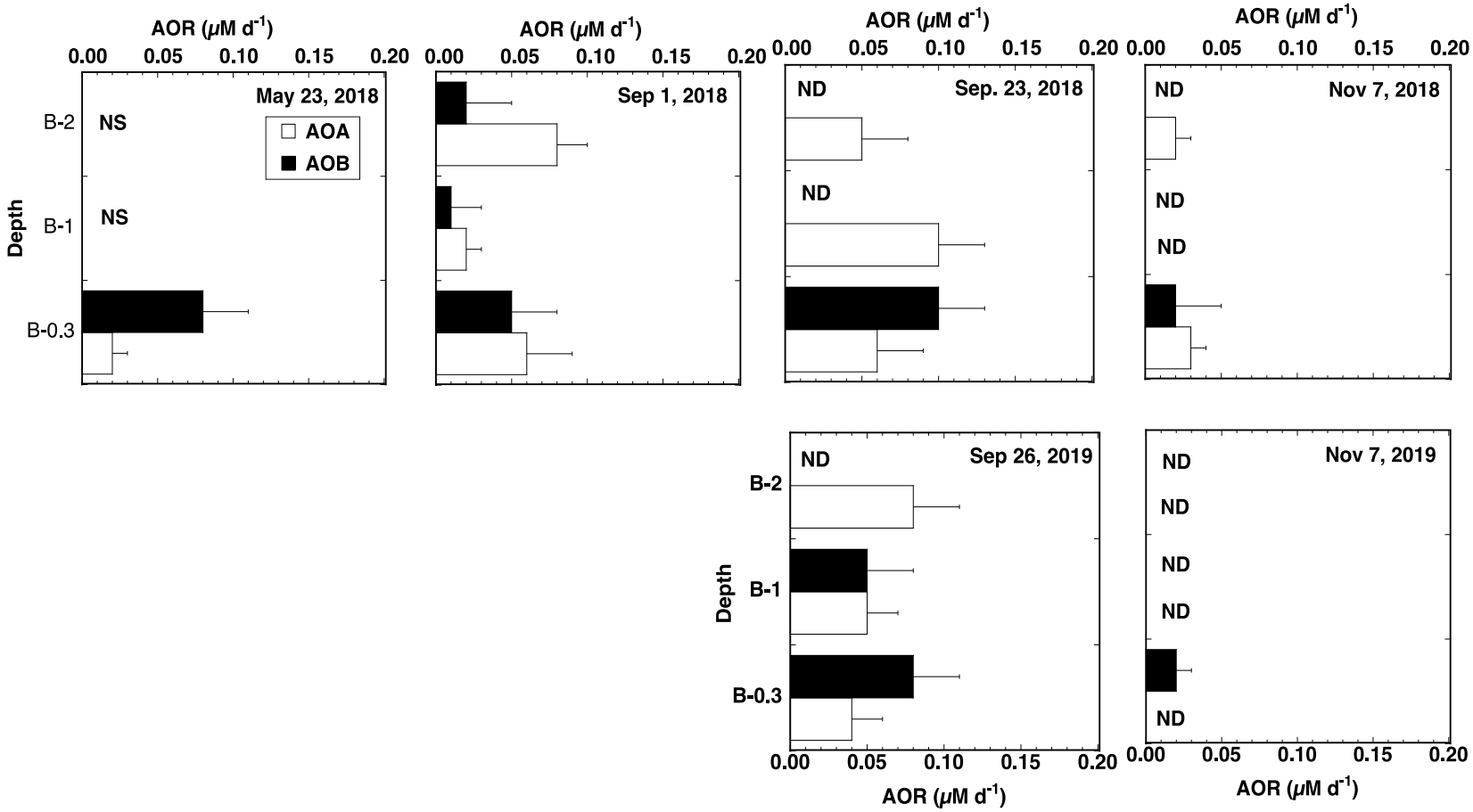
AOR (μM d-1)
0.00 0.05 0.10 0.15 0.20
May 23, 2018
Sep 1, 2018
Sep. 23, 2018
Nov 7, 2018
Sep 26, 2019
Nov 7, 2019
AOA
AOB
NS
ND
Depth
B-2
B-1
B-0.3

Fig. 5

1

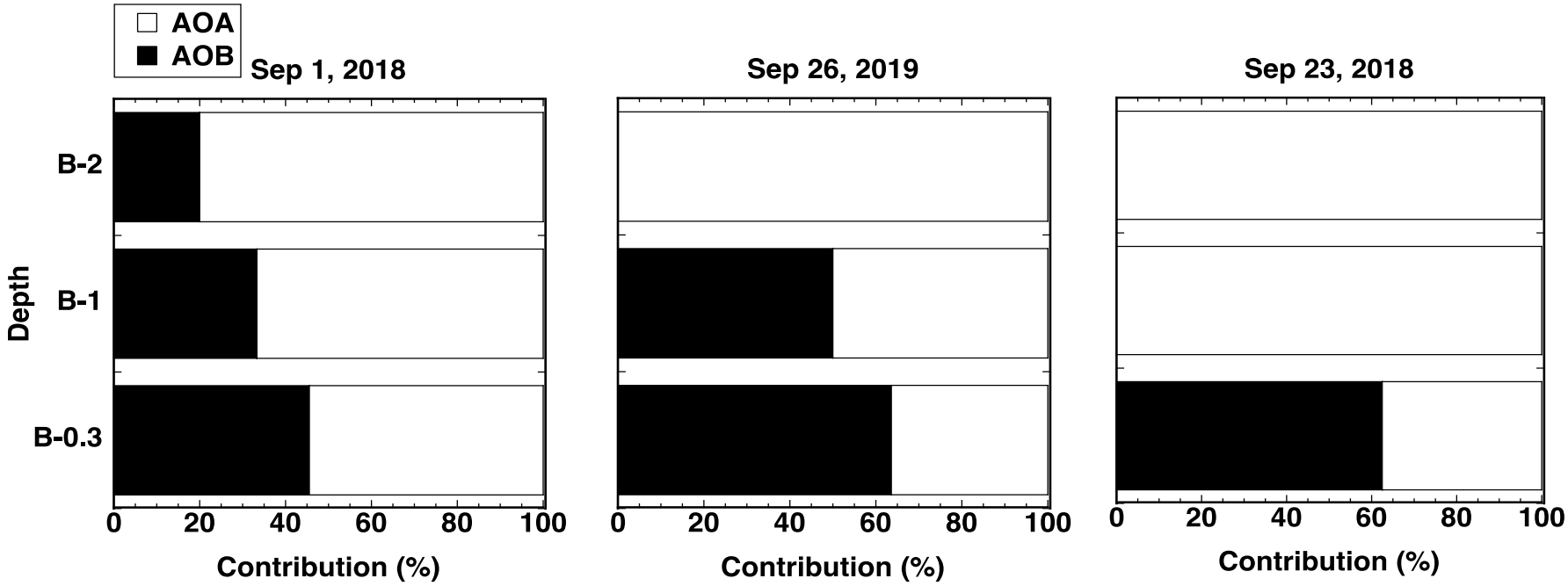
AOA
AOB
Sep 1, 2018
Sep 26, 2019
Sep 23, 2018
Depth
B-2
B-1
B-0.3
0
20
40
60
80
100
Contribution (%)

Fig. 6

1

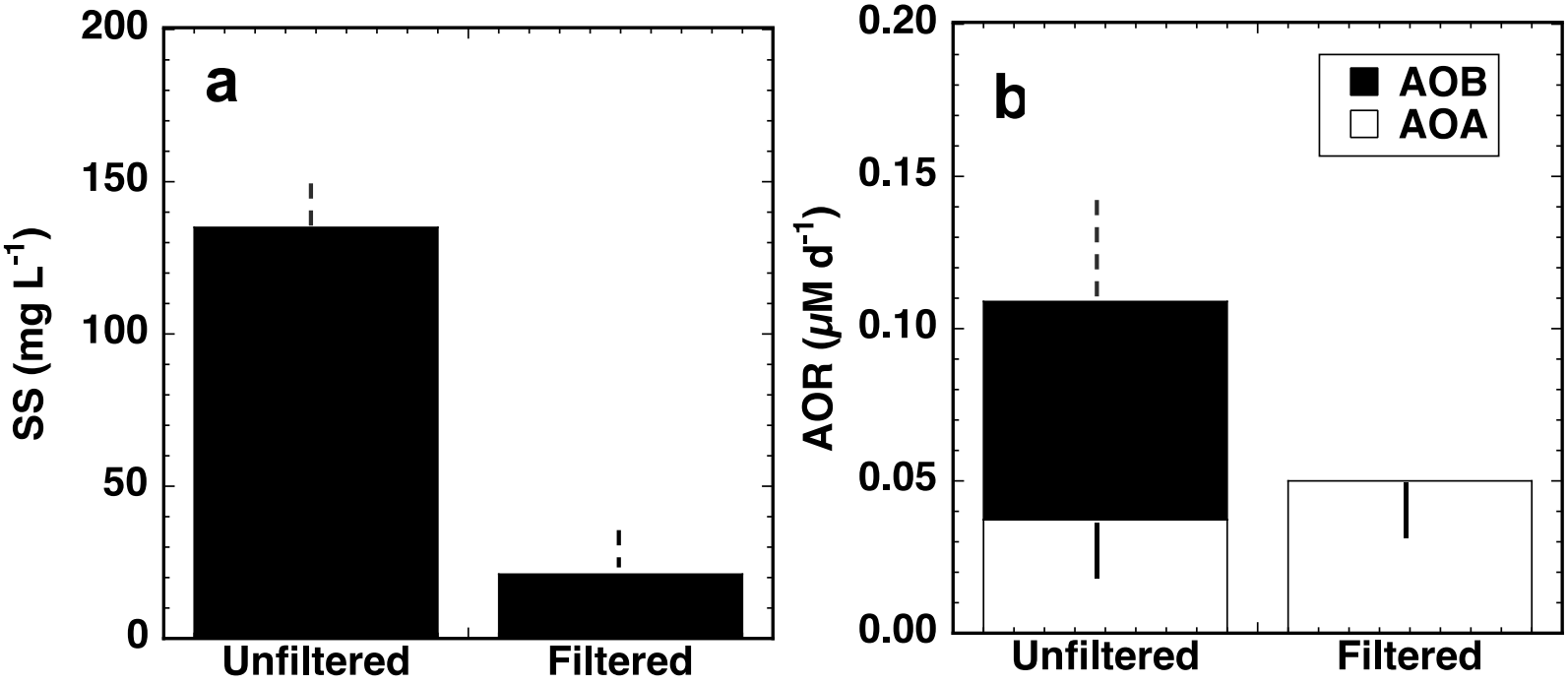
a
SS (mg L-1)
200
150
100
50
0
Unfiltered
Filtered
b
AOR (μM d-1)
0.20
0.15
0.10
0.05
0.00
AOB
AOA
Unfiltered
Filtered

Fig. 7

1

2

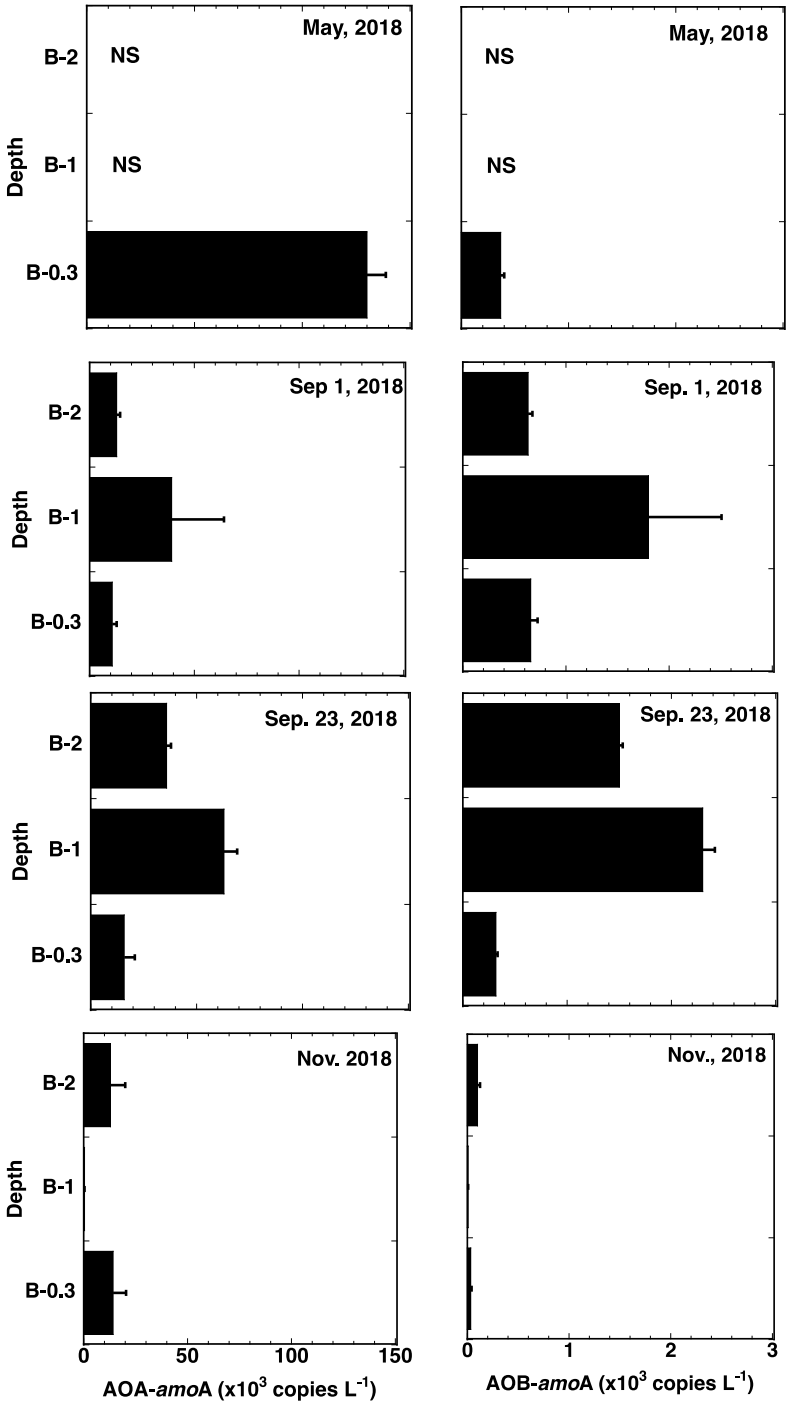
May, 2018
NS
NS
B-2
B-1
B-0.3
Depth
May, 2018
NS
NS
Sep 1, 2018
Sep. 1, 2018
Sep. 23, 2018
Sep. 23, 2018
Nov. 2018
Nov., 2018
0
50
100
150
AOA-amoA (x10^3 copies L^-1)
0
1
2
3
AOB-amoA (x10^3 copies L^-1)

Fig. 8

1
2

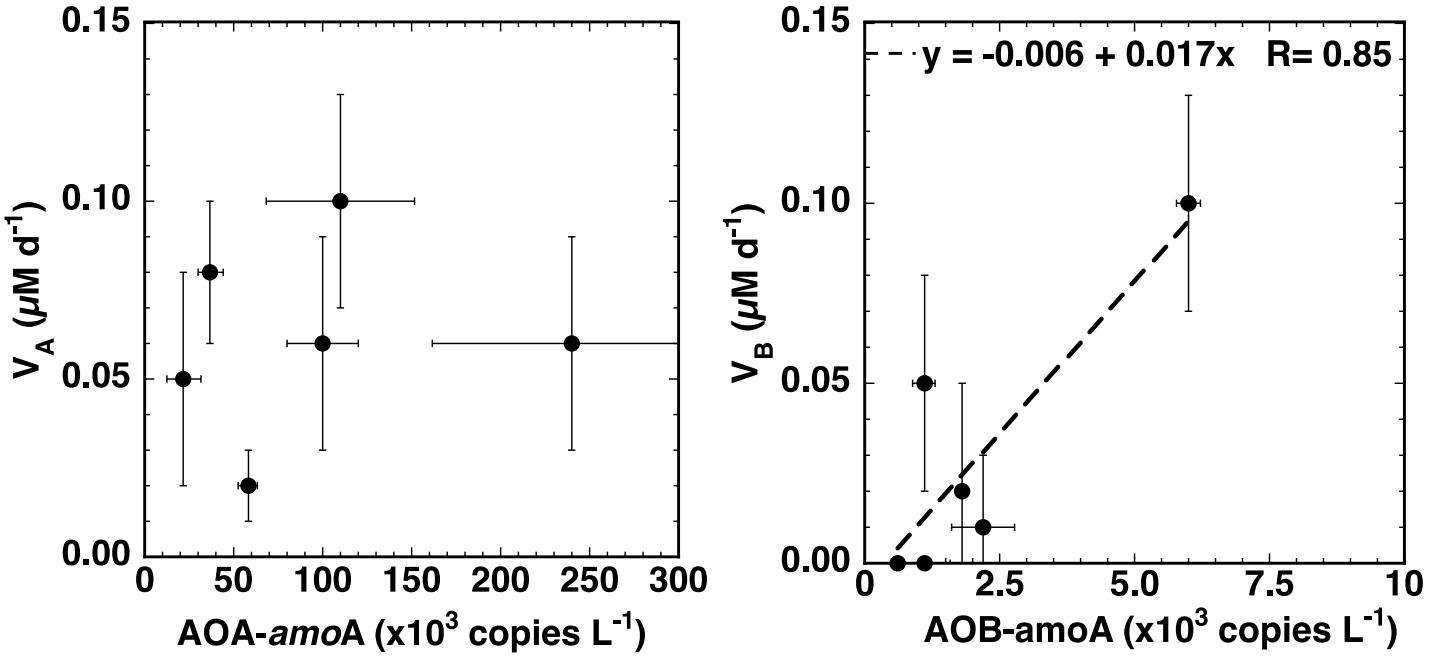
0.15
0.10
0.05
0.00
$V_A$ (μM $d^{-1}$)
0
50
100
150
200
250
300
AOA-*amo*A (x$10^3$ copies $L^{-1}$)
y = -0.006 + 0.017x R= 0.85
$V_B$ (μM $d^{-1}$)
0
2.5
5.0
7.5
10
AOB-amoA (x$10^3$ copies $L^{-1}$)

Fig. 9

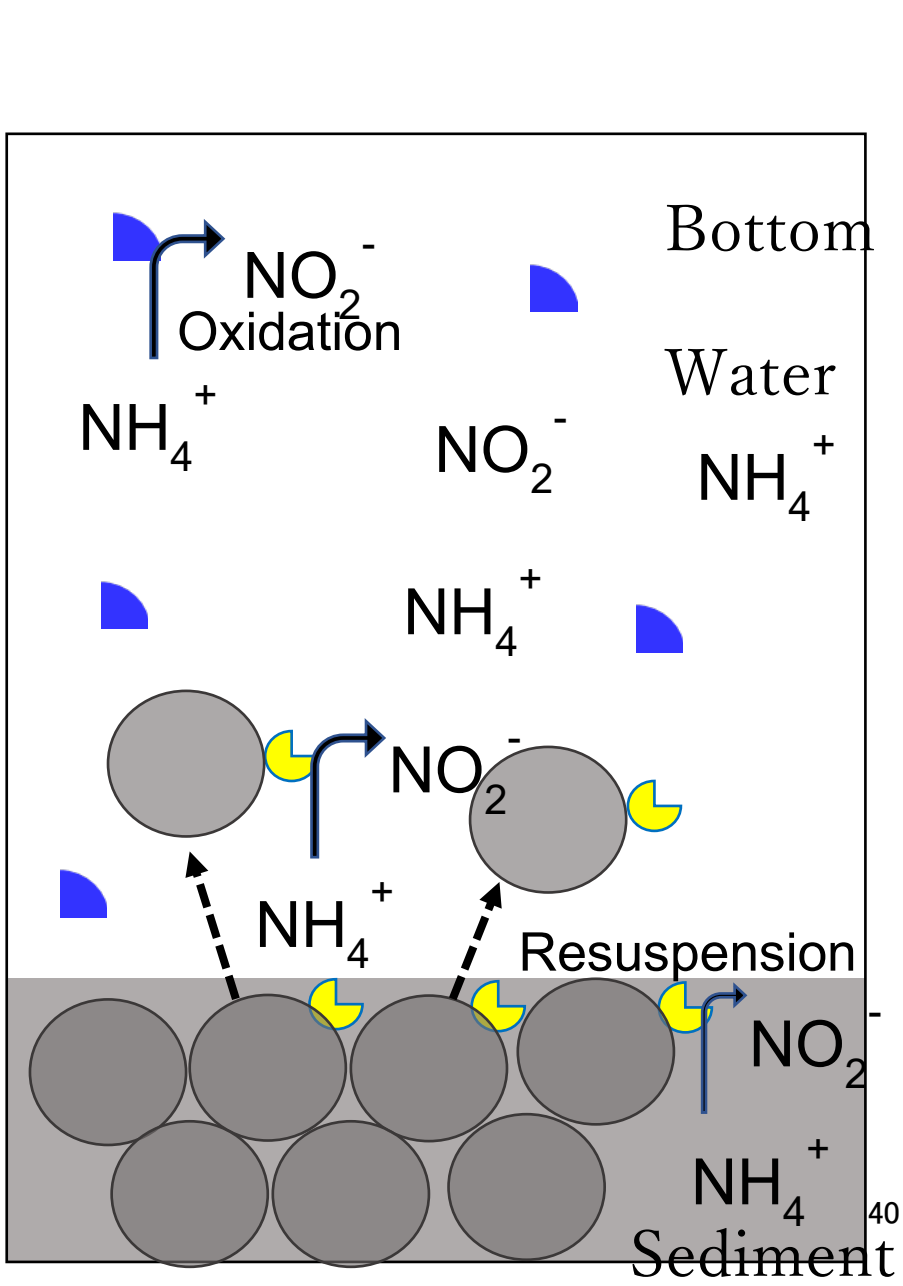
: Solid
: AOA
: AOB
Bottom
Water
Sediment
Oxidation
Resuspension
$NO_2^-$
$NH_4^+$

Fig. 10

Table 1 List of frequently used acronyms

| | |
|---|---|
| AOA | Ammonia Oxidizing Archaea |
| AOB | Ammonia Oxidizing Bacteria |
| AOOs | Ammonia Oxidizing Organisms |
| AOR | Ammonia Oxidation Rate |
| ATU | Allyl-thiourea |
| DIN | Dissolved Inorganic Nitrogen |
| PCR | Polymerase Chain Reaction |
| PNR | Potential Nitrification Rate |
| SS | Suspended Solids |

1

Table 2 Primers for q-PCR analysis

| Gene | Primer Set | Sequence 5'-3' | Length | Reference |
|---|---|---|---|---|
| AOA-amoA | crenAMO_F | ATGGTCTGGCTAAGACGMTGTA | 646 bp | Hallam et al. (2006) |
| | crenAMO_R | CCCACTTTGACCAAGCGGCCAT | | |
| AOB-amoA | AmoA-1F | GGGGTTTCTACTGGT | 491 bp | Rotthauwe et al. (1997) |
| | AmoA-2R | CCCCTCKGSAAAGCCTTCTTC | | |